


- Fully coherent all-sky CW searches computationally severely limited
 - » More efficient approach: **semicoherent searches**
(Divide data set into segments, each of which is coherently analyzed, then incoherently combine matched-filtering results from all segments)
- **Central problem:** design of and link between **coarse** and **fine** template grids
 - » Previous search methods used clever, but ad hoc constructions
- In recent work (HP & B. Allen, PRL, 2009), optimal **solution** to the incoherent combination problem found
 - » Key aspect: **new coordinates on parameter space**
- These coordinates allow the **first analytical parameter-space metric for the incoherent combination step.**
- Given this semicoherent metric, search codes can be improved to achieve a **significantly increased sensitivity** (e.g. for **Einstein@Home**)

Parameter-space metric of semicoherent searches for continuous gravitational waves



see poster:



Parameter-space metric of semicoherent searches for continuous gravitational waves

Holger J. Pletsch
Max Planck Institute for Gravitational Physics (Albert Einstein Institute), Hannover, Germany

Searching for CW sources

Rapidly rotating neutron stars are expected to generate continuous gravitational-wave (CW) signals via various mechanisms. Most such stars are electromagnetically invisible, but might be detected and studied via gravitational waves using LIGO-like detector instruments.

Matched filtering

A very powerful method to extract CW signals buried in the detector noise is based on maximum likelihood detection and leads to coherent matched filtering [3].

Doppler modulation

Rotating neutron stars emit monochromatic CW signals, apart from a slowly changing intrinsic frequency. But the terrestrial detector location Doppler-modulates the amplitude and phase of the waveform, as the Earth moves relative to the solar system barycenter (SSB).

The \mathcal{F} -statistic

Parameters describing the signal's amplitude variation may be eliminated by analytically maximizing the coherent matched-filtering statistic [1]. Thus, one explicitly searches only over phase parameter space \mathcal{P} , typically including the source's frequency f , frequency derivatives \dot{f} , \ddot{f} , and the sky location \hat{n} . The resulting coherent detection statistic is called the \mathcal{F} -statistic.

The novel approach

Answer: new coordinates on parameter space

The improved understanding of global parameter-space correlations yields new coordinates on \mathcal{P} . The new frequency and frequency derivative coordinates (up to second spin-down order \dot{f}) are [7]

$$\omega(t) = 2\pi f \left[f_0(t) + f_0(t) \hat{n} \cdot \hat{n} + f_0(t) \hat{n} \cdot \hat{n} \right], \quad (2)$$

$$\dot{\omega}(t) = 2\pi \dot{f} \left[\frac{f_0(t)}{f_0} + \frac{f_0(t)}{f_0} \dot{\hat{n}} \cdot \hat{n} + f_0(t) \dot{\hat{n}} \cdot \hat{n} + \frac{f_0(t)}{f_0} \dot{\hat{n}} \cdot \hat{n} \right], \quad (3)$$

$$\ddot{\omega}(t) = 2\pi \ddot{f} \left[\frac{f_0(t)}{f_0} + \frac{f_0(t)}{f_0} \ddot{\hat{n}} \cdot \hat{n} + \frac{f_0(t)}{f_0} \ddot{\hat{n}} \cdot \hat{n} + \frac{f_0(t)}{f_0} \ddot{\hat{n}} \cdot \hat{n} \right], \quad (4)$$

where $\hat{n}(t) = r_{\text{SSB}}(t)/r_{\text{SSB}}(t)$, with $r_{\text{SSB}}(t)$ denoting the vector from the Earth's barycenter to the SSB, and c the speed of light. The quantities $(\omega, \dot{\omega}, \ddot{\omega})$ are called the **global-correlation parameters** [7], because they describe the global correlation hypersurfaces at the corresponding order of \mathcal{F} . They can be interpreted as the source's instantaneous frequency and frequency derivative of the Earth's center, at time t . It is useful to also introduce new (real-valued) sky coordinates n_x and n_y [2a], [8], given by

$$n_x(t) = f_0(t) \hat{n} \cdot \hat{n} = 2\pi f_0(t) \cos \theta \cos \phi \cos \psi, \quad (5)$$

Here $r_x = R_E/c \approx 23$ ms is the light travel time from the Earth center to the detector, and $r_{\text{SSB}}(t)$, $\dot{r}_{\text{SSB}}(t)$, $\ddot{r}_{\text{SSB}}(t)$ are the detector position at time t . The resulting phase model $\Phi(t)$ is linear in $(\omega, \dot{\omega}, \ddot{\omega}, n_x, n_y)$:

$$\Phi(t) = \omega(t) \left(\frac{t-t_0}{T} \right) + \dot{\omega}(t) \left(\frac{t-t_0}{T} \right)^2 + \ddot{\omega}(t) \left(\frac{t-t_0}{T} \right)^3 + n_x(t) \cos(2\pi \nu) + n_y(t) \sin(2\pi \nu), \quad (6)$$

at reference time t_0 . This phase model is a good approximation for $T \lesssim 1$ week, when ν is included as a search parameter [5, 7].

Simulated CW signal

To illustrate the results predicted by the semicoherent metric a data set containing a simulated CW signal is prepared and analyzed. The simulated data set, referring to the LIGO H1 detector, consists of $N = 111$ segments of duration $T = 25$ s, and spans about 1 year.

Coherent stage

Data segment 1 of 111
This figure shows the \mathcal{F} -statistic projected onto the 2D subspace of frequency and first spin-down order for the first data segment. The color bar indicates the values of \mathcal{F} .
The location of the simulated CW signal is denoted by the intersecting white dashed lines.

Data segment 28 of 111
As also seen in the previous plot, the iso-mismatch contours in \mathcal{F} -statistic are very elongated in one direction. This allows to use coarse template grids in the coherent stage, with coarse spacings along the elongated direction.

Data segment 56 of 111
In this figure, the data segments are aligned with the reference time t_0 . Therefore, the metric eigenvectors are aligned with the coordinate axes as described by Eq. 10. The green dashed contours indicate the 10% coherent-metric mismatch.

Data segment 84 of 111
These plots also demonstrate that at local reference time t_0 , for data segments further away from t_0 , the iso-mismatch contours in \mathcal{F} -statistic are being stretched and rotated around the signal location. The metric determined is independent of t_0 . Hence, the rotating and stretching happens at constant iso-mismatch-ellipse area.

Data segment 111
This figure shows the \mathcal{F} -statistic for the last segment. The next stage combines the coherent results from all segments incoherently, mapping each coarse grid to the fine grid via the metric Eq. (6). The fine-grid construction is governed by the semicoherent metric Eq. (10).

Semicoherent combination stage

Here the color code shows the average \mathcal{F} -values obtained from combining the 111 segments.
The green dotted ellipse indicates the 10% semicoherent metric mismatch region, as described by Eq. (10). The metric prediction does well agree with contours obtained from the full signal simulation.

First analytical semicoherent metric

Coherent metric

The metric for the coarse grid of the coherent stage (\mathcal{F} -statistic) for the j th segment is determined from

$$g_{\mu\nu}^{(j)} = \langle \partial_\mu \Phi_j \partial_\nu \Phi_j \rangle = \langle \partial_\mu \Phi_j \partial_\nu \Phi_j \rangle, \quad (7)$$

where $\langle \dots \rangle \equiv \int_{\mathcal{P}} \dots \mathcal{P}(t) dt$ is the time average over the j th segment spanning $[T_j, T_j + T]$. The components of $g_{\mu\nu}^{(j)}$ consistently simplify if the reference time t_0 is chosen as $t_0 = T_j - 3$ and T is taken to be a positive integer number q of sidereal days [8].

$$g_{\mu\nu}^{(j)} = \begin{pmatrix} \frac{1}{2} & 0 & 0 & 0 & 0 \\ 0 & \frac{1}{2} & 0 & 0 & 0 \\ 0 & 0 & \frac{1}{2} & 0 & 0 \\ 0 & 0 & 0 & \frac{1}{2} & 0 \\ 0 & 0 & 0 & 0 & \frac{1}{2} \end{pmatrix} \quad (8)$$

with the constant components $A(t) = \pm 1/2 \nu$, $B(t) = \pm 1/2 \nu^2$, and $C(t) = \pm 1/2 \left[\frac{1}{2} + \frac{1}{2} \frac{1}{\nu^2} \right]$. The above metric is explicitly coordinate-independent (proving that \mathcal{P} is flat). In fact, the region around a point p in which the mismatch \mathcal{M} is well approximated is much larger using $(\omega, \dot{\omega}, \ddot{\omega}, n_x, n_y)$.

Semicoherent metric

The incoherent step combines the coherent analysis results from the N segments labeled by $j = 1, \dots, N$. The spacing of the fine grid is determined from the semicoherent metric $\tilde{g}_{\mu\nu}$ for the fractional loss of the expected \mathcal{F} -statistic, \mathcal{F}_j . One can show [2, 9]

$$\tilde{g}_{\mu\nu} = \frac{1}{N} \sum_{j=1}^N g_{\mu\nu}^{(j)} \quad (9)$$

The most convenient choice of reference time t_0 is given by $t_0 = \frac{1}{N} \sum_{j=1}^N T_j$ [6]. To further simplify the metric components, T is again taken to be a positive integer number q of sidereal days. Thus:

$$\tilde{g}_{\mu\nu} = \begin{pmatrix} \frac{1}{2} & 0 & 0 & 0 & 0 \\ 0 & \frac{1}{2} & 0 & 0 & 0 \\ 0 & 0 & \frac{1}{2} & 0 & 0 \\ 0 & 0 & 0 & \frac{1}{2} & 0 \\ 0 & 0 & 0 & 0 & \frac{1}{2} \end{pmatrix} \quad (10)$$

where $A(t) = \pm 1/2 \nu$, $B(t) = \pm 1/2 \nu^2$, and $C(t)$ denotes the **central moment of the data segment's "distribution"** (t_j) , $\tilde{g}_{\mu\nu} = \frac{1}{N} \sum_{j=1}^N \left(\frac{t_j - t_0}{T} \right)^2$ [6]. From Eq. (10) follows that **only the spin-down metric components need to be refined with constant [1]**. Thus, one may define the template-grid refinement factor ν_{ref} for 3 spin-down parameters as

$$\nu_{\text{ref}} = \sqrt{\frac{\tilde{g}_{\mu\nu}}{g_{\mu\nu}^{(j)}}} = \sqrt{\frac{2000(\tilde{g}_{\mu\nu} - \beta_{\mu\nu}^2)}{\beta_{\mu\nu}^2}} \approx N^2, \quad (11)$$

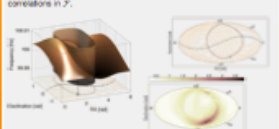
where $\nu_{\text{ref}} = \sqrt{1 - \frac{1}{N}}$ corresponds to the 1-spin-down case.

Global correlations

The \mathcal{F} -statistic has strong global correlations in the physical coordinates $(f, \dot{f}, \ddot{f}, \hat{n})$, extending outside a region in which \mathcal{M} is well approximated by the local metric above [4, 7].

Global parameter-space correlations in \mathcal{F} -statistic

Given a signal, the region where the expected \mathcal{F} -statistic has maximal value may be described by a separate equation for each order of \mathcal{F} , when T is small compared to one year. The solutions [7] to each equation is a **hypersurface**, whose intersections describe the global correlations in \mathcal{F} .



Second-order in T non-negligible

For currently used values of T (a day or longer) it is also crucial to consider the fractional loss and global structure of \mathcal{F} to second-order in T .

References

- [1] P. Jaranowski, et al., Phys. Rev. D 58, (1998).
- [2] P. R. Brady et al., Phys. Rev. D 57, 1169, and 61, (2000).
- [3] C. Cullen, et al., Phys. Rev. D 72, (2005).
- [4] R. Prix and Y. Itoh, Class. Quant. Grav. 22, (2005).
- [5] P. Assen et al., Phys. Rev. D 65, (2002).
- [6] B. Krishnan et al., Phys. Rev. D 70, (2004).
- [7] H. J. Pletsch, Phys. Rev. D 79, (2009).
- [8] H. J. Pletsch and B. Allen, Phys. Rev. Lett. 103, (2009).
- [9] H. J. Pletsch, in preparation, LIGO-P1000065-v1, (2010).
- [10] <http://www.ligo.org>